



You have downloaded a document from
RE-BUŚ
repository of the University of Silesia in Katowice

Title: Pb-Rich Slags, Minerals, and Pollution Resulted from a Medieval Ag-Pb Smelting and Mining Operation in the Silesian-Cracovian Region (Southern Poland)

Author: Jerzy Cabała, Rafał Warchulski, Dariusz Rozmus, Dorota Środek, Eligiusz Szełęg

Citation style: Cabała Jerzy, Warchulski Rafał, Rozmus Dariusz, Środek Dorota, Szełęg Eligiusz. (2020). Pb-Rich Slags, Minerals, and Pollution Resulted from a Medieval Ag-Pb Smelting and Mining Operation in the Silesian-Cracovian Region (Southern Poland). "Minerals" (Vol. 10 (2020), Art. No. 28), doi 10.3390/min10010028



Uznanie autorstwa - Licencja ta pozwala na kopiowanie, zmienianie, rozprowadzanie, przedstawianie i wykonywanie utworu jedynie pod warunkiem oznaczenia autorstwa.



UNIwersYTET ŚLĄSKI
W KATOWICACH



Biblioteka
Uniwersytetu Śląskiego



Ministerstwo Nauki
i Szkolnictwa Wyższego

Article

Pb-Rich Slags, Minerals, and Pollution Resulted from a Medieval Ag-Pb Smelting and Mining Operation in the Silesian-Cracovian Region (Southern Poland)

Jerzy Cabała^{1,*}, Rafał Warchulski¹, Dariusz Rozmus², Dorota Środek¹ and Eligiusz Szełęg¹

¹ Faculty of Natural Sciences, University of Silesia, Bedzinska 60 Street, 41-200 Sosnowiec, Poland; rafal.warchulski@us.edu.pl (R.W.); dorota.srodek@us.edu.pl (D.Ś.); eligiusz.szeleg@us.edu.pl (E.S.)

² The City Museum "Szttygarka", Legionów Polskich 69, 41-300 Dąbrowa-Górnicza, Poland; rozmusd@poczta.onet.pl

* Correspondence: jerzy.cabala@us.edu.pl

Received: 25 November 2019; Accepted: 24 December 2019; Published: 28 December 2019



Abstract: Since the 12th century in the Silesian-Cracovian area, lead, litharge, and silver have been produced by the pyrometallurgical processing of Pb-Ag-Zn ore. Slags and soils contaminated with heavy metals (Zn, Pb, Cd, Fe, Mn, As) were the subject of this research. Samples were collected during archaeological works in the area of early medieval metallurgical settlement. The main goals of the analyses (Scanning Electron Microscopy-Energy Dispersive Spectroscopy (SEM-EDS), Electron Probe Microanalyzer (EPMA), X-ray diffraction (XRD), Atomic Absorption Spectroscopy (AAS)) were the determination of the mineralogical composition of furnace batches and smelting temperatures and conditions. In soils, the anthropogenic phases enriched in Pb, Zn, Fe, Mn, P, and primary minerals like goethite, ferrihydrite, sphalerite, galena, smithsonite, minrecordite, cerussite, gypsum, anglesite, jarosite, and hemimorphite were identified. The soil from former metallurgical settlements contained up to 1106 mg·kg⁻¹ Pb, 782 mg·kg⁻¹ Zn, 4.7 mg·kg⁻¹ Cd in the fine fraction. Much higher heavy metal concentrations were observed in the waste products of ore rinsing, up to 49,282 mg·kg⁻¹ Pb, 64,408 mg·kg⁻¹ Zn, and 287 mg·kg⁻¹ Cd. The medieval smelting industry and Pb-Ag-Zn ore processing are marked by highly anomalous geochemical pollution (Pb, Zn, Cd, Fe, Mn, Ba) in the topsoil. The methods of mineralogical investigation, such as SEM-EDS or EMPA, can be used to identify mineralogical phases formed during metallurgical processes or ore processing. Based on these methods, the characteristic primary assemblage and synthetic phases were identified in the area polluted by medieval metallurgy and mining of Pb-Ag-Zn ores, including MVT (Mississippi Valley Type) deposits. The minerals distinguished in slags and the structural features of metal-bearing aggregates allow us to conclude that batches have included mostly oxidised minerals (PbCO₃, ZnCO₃, CaZn(CO₃)₂, FeOOH), sulfides (PbS and ZnS) and quartz (SiO₂). The laboratory experiment of high-temperature heating of the examined slags showed that smelting temperatures used in the second half of 13th century were very high and could have reached up to 1550 °C. The results indicate, that geochemical and mineralogical methods can be used to obtain important information from archaeological sites, even after archaeological work has long ceased.

Keywords: Pb-rich slags; soil contamination; historical Zn-Pb mining; secondary Zn-Pb minerals

1. Introduction

In medieval Europe, the development of countries and power centres was often connected with the sourcing and utilization of mineral resources. Non-ferrous minerals played an important role. The proximity of iron, gold, silver, lead, copper and tin deposits has promoted the development of

mining and metallurgy centres since Roman times. In the period between the 10th and 12th centuries, iron, lead, tin, silver, and gold had become more important for the development of civilization in Central and Eastern European countries. Since the beginning of the 10th century in medieval Europe, in areas where ores of Ag-Pb, Au, As-Au, Cu, Sn and Fe occur, mining centres have appeared, such as at the Ore Mountains (Erzgebirge), Harz Mountains, and Sudetes.

One of Europe's largest Zn-Pb, MVT (Mississippi Valley) type ore deposits can be found in the Silesian-Cracow area (southern Poland) [1]. Shallow deposits are represented by supergene type Zn-Pb of ores [2]. The deposit's location has been advantageous for the development of the silver and lead mining in the 12th century, which is confirmed by historical sources and archaeological research [3]. In the vicinity of the mining sites, lead and silver metallurgy centres arose. It can be assumed that the metallic deposit exploitation begun taking place in the 10th and 11th centuries, due to the fact that at the same time mining settlements and cities, such as Bytom, Olkusz or Tarnowskie Góry began. The beginnings of these cities were associated with mining. The metallurgical settlements, places of processing, and rinsing of Pb-Ag ore and multiple artefacts, for the production of which lead, litharge or silver has been used, were found in the area of Olkusz, Siewierz, and Łosień (near Dabrowa Gornicza) (Figure 1) [4,5].

In one of these localities, between 2003 and 2007, archaeological research was carried out. Subsequently, the surface was levelled, restored to the previous condition, and returned to the owner. It has been assumed that, due to several years of archaeological investigation and the subsequent backfilling of the sediment layer on the excavation site, it would be possible to analyse the surface material for mineral grains originating in furnace batch materials, slags, or even the final products of the metallurgical processes undertaken there.

The geochemical investigation of metallurgical slags can be the source of important data for archaeometallurgy, knowledge of historical environmental pollution and regional geology [6–9]. The historical metallurgical slags are good materials for providing information on former metal smelting methods and their contemporary mining ore quality [10–14]. The examination of slags can provide significant information about chemical transformation rates and the metal stability associated therein [15–20]. Multiple geochemical investigations show that, historically, lead production has had an impact on environmental pollution since the Roman times, e.g., in England [21], Sweden [22], and Spain [23]. Metal transfer from the waste to the environment can occur even for several hundred years after the end of metallurgy or mining [24,25].

Medieval lead and silver metallurgy is studied using mineralogical investigations of slags in France [26], Czech Republic [11,27], Germany [10], Italy [28]. There is relatively little data about medieval Pb-Ag early metallurgy in the Silesian-Cracow region (Southern Poland). Information about the exploitation scale, enrichment methods and Pb and Ag production technologies is mostly unavailable. On the other hand, the investigations of early-medieval metallurgical products and artefacts made from lead, which were found in different parts of Europe, show that the source for their production was galena from Silesian-Cracow ores [11].

The main goal of this research was proving if scanning electron microscopy with energy dispersive spectroscopy (SEM-EDS), electron-probe microanalyser (EPMA), or X-ray diffraction (XRD) results obtained from material collected at previously investigated archaeological sites could be useful for analysing the input material type, metallurgical methods, and degree of environmental pollution. The identification of mineralogical and chemical composition of medieval lead and silver metallurgy products and wastes should provide important information about the methods of obtaining metals and their compounds (e.g., litharge). An important aspect of this research is the degree to which soil is polluted by Pb, Zn, Cd, and Tl in the area of medieval metallurgical settlements, and the recognition of geochemical metal-bearing mineral activity.

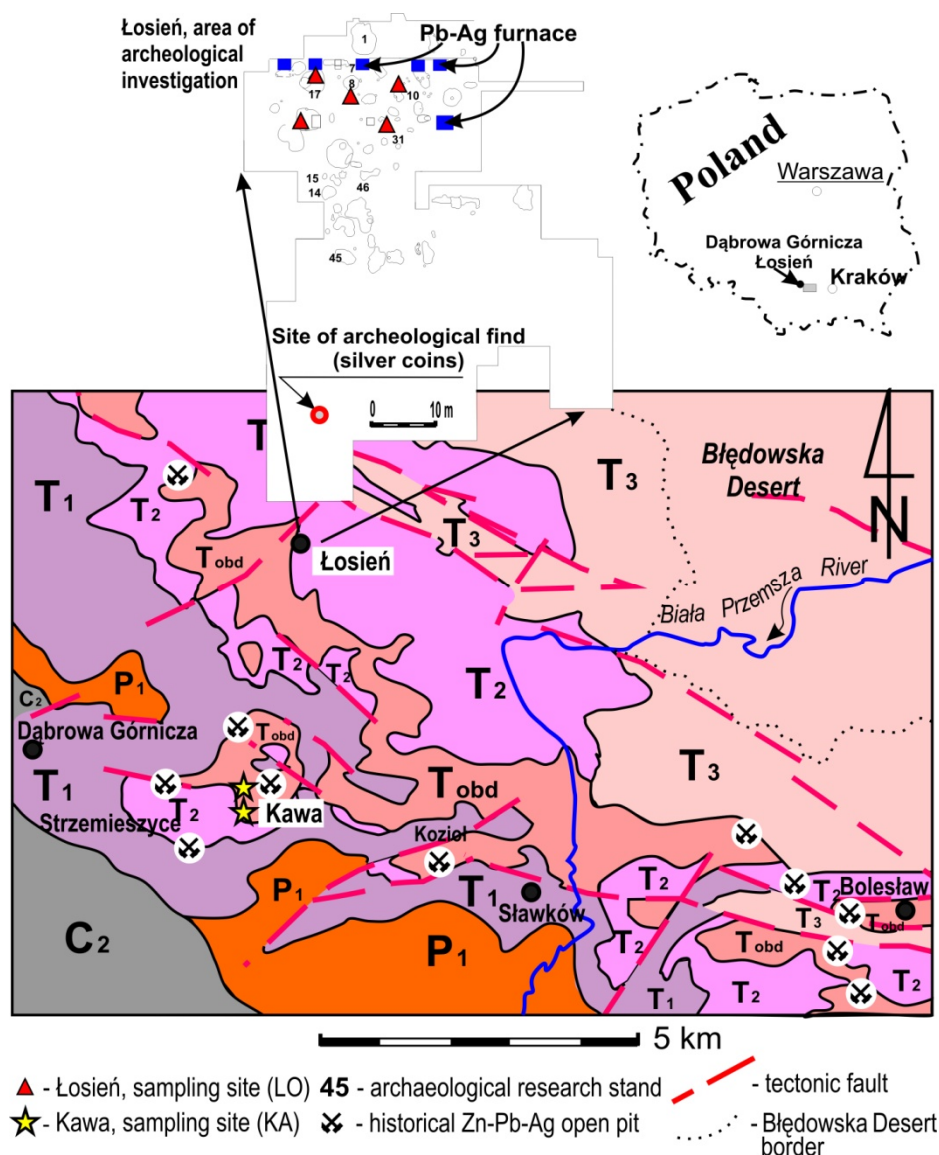


Figure 1. Geological sketch of the study area (without Pleistocene deposits). Explanations: C2—Upper Carboniferous—USCB border, P1—Lower Permian, T1—Lower Triassic, T2—Middle Triassic, T3—Upper Triassic, Tobd—Ore-bearing dolomites with Zn-Pb-Ag mineralization.

2. Study Site, Geological and Archeological Data

2.1. Study Site

The research site lies in Southern Poland, in the Silesian-Cracow area, where Zn-Pb ores of Mississippi Valley Type (MVT) occur [29,30]. The research area was an archaeological site in Łosień (near Dąbrowa Górnicza), where forges for lead and silver smelting, ceramics and other artefacts (e.g., coins) dated at 1165–1180 were found (Figure 1). The second research area is the mining grounds and former Zn-Pb-Ad ore mud in Kawa (near Dąbrowa Górnicza), which lies at the ore deposit outcrop.

2.2. Geological Setting

The Zn-Pb and Pb-Ag ores are found in epigenetic metalliferous dolomite from the Middle Triassic. The ore-bearing horizons are shallow, and they outcrop at the surface [30,31]. Triassic limestones, dolomites, and silts form the surface morphology, and locally they are covered by residual rock, waste

sediment, and Pleistocene fluvioglacial sands. On carbonate formations, Rendzina-type soils are developed, while on sands, podzols occur.

2.3. Archeological Data

In the area of small morphological thresholds, shallow (up to 1 m) archaeological work was carried out in 2004–2007 (Figure 1). The works were successful, with six lead and silver smelting furnace localities discovered, several dozen silver spots, with a total weight of 1.5 kg, and numerous fragments of clay vessels found. The most spectacular discovery was a clay pot with over 1100 silver coins, dated at 1165–1180 [32]. These were probably the remnants of an early-medieval metallurgical settlement, which had been hastily abandoned. The second examined area (Dąbrowa Górnicza-Kawa) is four kilometers away, and shallow Zn-Pb-Ag deposits are present there. Lead ore used at a medieval smelter could have come from these deposits. At this site, fragments of Zn-Pb ores from 19th century were found.

3. Materials and Methods

3.1. Sampling

Five 1-kg samples were collected from 0–0.05 m of topsoil in two locations. The samples come from surface, formed during backfilling and levelling the area after archaeological work in the discovered smelting furnace at the Łosień site (Samples named LO). Samples from Kawa (marked as KA) were collected in the area where historical Zn-Pb ores exploitation and ore washing was taking place. Soil components were separated into grain size fractions $>63 \mu\text{m}$, $40\text{--}63 \mu\text{m}$ and $<40 \mu\text{m}$. The sampling area was marked on the map (Figure 1).

3.2. Petrology and Geochemistry

The contaminated soil and fragments of slag were hand-picked and mounted in resin for scanning electron microscope-energy dispersive spectroscopy (SEM-EDS) studies. These studies were carried out using an environmental scanning electron microscope Philips XL 30 with EDAX analyser. Back scattered electron (BSE) images were obtained using a Centaurus attachment with a detector resolution of 0.3 Z. The accelerating voltage was 15 kV. Analyses were performed in environmental- and low-pressure (0.3 Torr) modes. EDS spectra analyses were obtained using Phillips software.

Electron probe micro-analyses (EPMA) were performed using a CAMECA SX 100 electron microprobe (Inter-Institutional Laboratory of Microanalysis of Minerals and Synthetic Materials, University of Warsaw, CAMECA, Gennevilliers, France). Analyses were performed at 15 keV accelerating voltage, a 10–20.1 nA beam current, and a beam diameter of up to $5 \mu\text{m}$. Standards included: Al–KAlSi₃O₈, As–GaAs, Ca–CaSiO₃, Fe–Fe₂O₃, K–KAlSi₃O₈, Mg–MgCaSi₂O₆, Mn–MnCO₃, P–Ca₅(PO₄)₃(F, Cl, OH), Pb–PbS, PbCrO₄, S–BaSO₄, CuFeS₂, ZnS, Si–CaSiO₃, Zn–ZnS.

X-ray powder diffraction data were obtained using a PANalytical X'PERT PRO–PW 3040/60 diffractometer (Malvern Panalytical Ltd, Malvern, UK) (CuK α 1 source radiation, Ni-filter to reduce the K β radiation, and X'Celerator detector), at the Faculty of Earth Sciences, University of Silesia (Katowice, Poland). Quantitative data processing was performed by means of the X'PERT High Score Plus software using the latest PDF4+ database.

Heavy metal contents (Zn, Pb, Fe, Mn, Cd, and Tl) were analysed by atomic absorption spectroscopy (AAS) using a SOLAAR spectrometer (M6 v. Thermo Scientific, USA). All BSE, EDS, and AAS analyses were carried out in the laboratories of the Faculty of Earth Sciences, University of Silesia, Sosnowiec.

3.3. Experiments

Slags are the waste material resulting from the necessity of binding possible impurities within, most commonly, silicate melt. As such, they are completely molten during the smelting process, and thus heating experiments leading to remelting slag samples can be used to approximate the

minimum temperature during the smelting process. Experiments were performed in the chamber furnace PLF 160/5 with PC 442/18 controller (manufacturer Protherm Furnaces, Ankara, Turkey), SiC heaters and Thermocouple S with a maximum working temperature of 1550 °C. Samples were melted and crystallized in alumina pots and oxidizing conditions. To determine the melting temperature of the slag samples, we performed successive experiments with rising temperatures and fast cooling, until a complete melting of the sample (1 cm³) occurred.

4. Results

4.1. Soil Phase Composition

4.1.1. XRD Studies

The areas contaminated by historical Pb-Ag and Zn-Pb-Fe ore processing are characterised by a unique mineral assemblage (Table 1).

Table 1. Mineral phases detected by selective XRD analysis.

| Phase | Site | | |
|---------------------------|--|--|--|
| | Pb-Ag Smelting, (12th Century) Łosień (LO) | Zn-Pb Washing Historical Wastes Kawa (KA) | Zn-Pb Mining, Historical Wastes Kawa (KA) |
| Barren phase | illite, quartz, calcite, dolomite | dolomite, ankerite, calcite, illite, quartz, K-feldspar, | dolomite, calcite, quartz, ankerite, K, Na- feldspar, illite, kaolinite |
| Major metalliferous phase | litharge, cerussite, goethite | cerussite, smithsonite, goethite, galena | goethite, ferrihydrite, sphalerite, galena, smithsonite, minrecordite, cerussite, barite |
| Minor phase | magnetite, barite, SiO ₂ , glassy silica, pyromorphite, metallic Pb, Pb slag, Ti oxide, mullite | Ca phosphate, Fe-Mn oxide, Mn oxide | gypsum, anglesite, jarosite, hemimorphite, magnetite |

At the early-medieval lead and silver smelting site, Pb-bearing minerals represented by carbonates (cerussite, PbCO₃) and oxides (litharge, PbO) occur. Metallic Pb, barite (BaSO₄), silicate glass, and slags with Pb and PbO were also identified. The synthetic aluminosilicates (e.g., mullite 3Al₂O₃·2SiO₂) and Pb phosphates with chemical composition close to the pyromorphite (Pb₅(PO₄)₃Cl) were recognized as well.

The areas where the Zn-Pb ore washing process took place, are characterized by the occurrence of oxidized Zn, Pb and Fe carbonated minerals (Table 1). Smithsonite (ZnCO₃) and cerussite with co-occurring Fe-oxides (goethite, Fe³⁺O(OH)) are dominant. The Mn-Fe and Mn oxides and Ca phosphates are much less common.

In areas of the historical Zn-Pb-Ag ore mining, dolomite and calcite with significant ankerite and clay mineral additives are the main minerals. The metal-bearing minerals are represented by goethite and Fe hydroxides, mostly. Sphalerite, galena, carbonate minerals such as smithsonite, cerussite, and minrecordite (Ca,Zn(CO₃)₂) were identified as well. Barite is present in the assemblage with Zn and Pb sulfides. Hemimorphite Zn₄Si₂O₇(OH)₂·(H₂O), magnetite Fe₃O₄ and sulfates: gypsum (CaSO₄·2H₂O), anglesite (PbSO₄) and jarosite (KFe³⁺₃(SO₄)₂(OH)₆) are present in much less significant quantities.

4.1.2. SEM-EDS Studies

Areas of medieval smelter operation (Łosień)

In topsoil, mineralogical composition from medieval Pb-Ag smelting industry sites, submicroscopic-size phases containing heavy metals such as: Pb, Zn, Fe, Mn, Cd, Ba occur. In fine-grained fractions, polymineralic, lead-rich aggregates are present (Figure 2a–c). The EDS microanalyses show that these are Pb oxides together with Ca aluminosilicates (Figure 2a). They form dense, slightly cracked grains

with sharp edges up to 150 μm in size. Grains of fine-crystalline Pb carbonate (up to 50 μm in size) were identified as well. At the irregular surface, Zn aluminosilicates are present (Figure 2b).

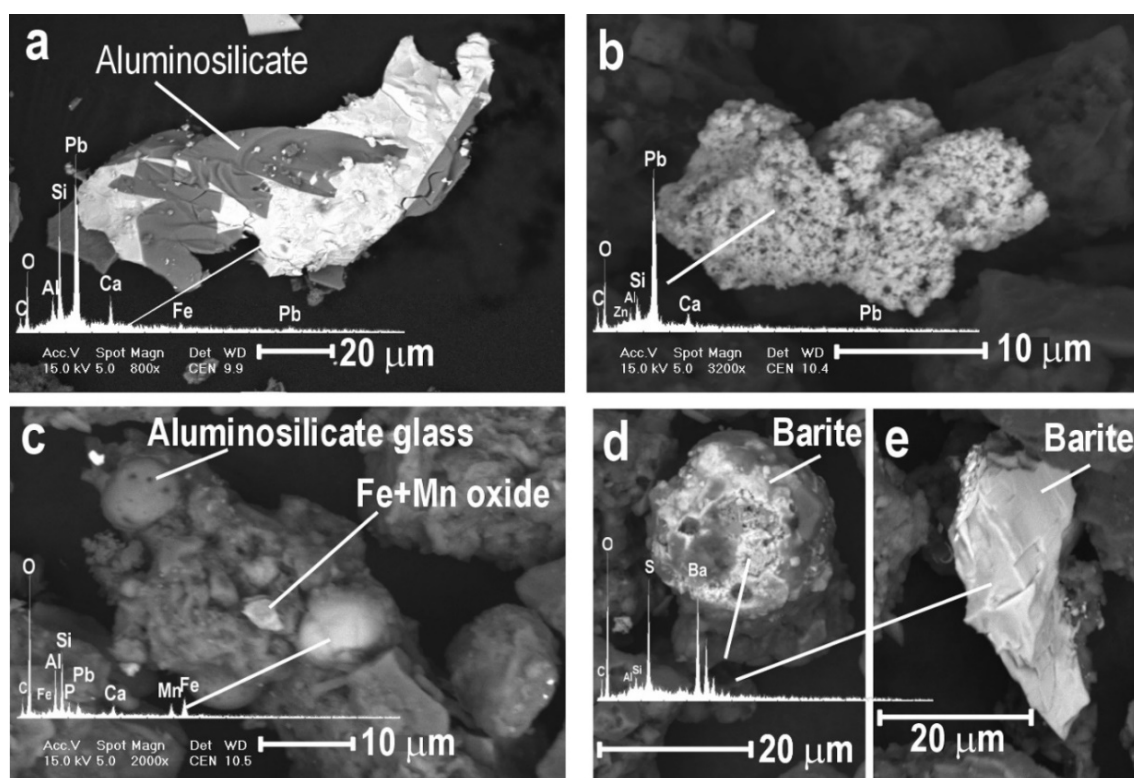


Figure 2. BSE images of metal components in the topsoil from areas of archaeological investigation of medieval Ag-Pb smelting operations. (a) Aggregates Pb-oxides and aluminosilicates. (b) Microporous grain Pb carbonate. (c) polymineral aggregate with Fe and Mn oxide, Pb-phosphate and Fe-Mn-oxide. (d) Barite transformed by melting. (e) Barite in crystal form.

Soils contaminated by the medieval smelting industry are characterized by the presence of polymineralic aggregates with complicated chemical formulas. Such aggregates are formed by small (up to 10 μm in size) isometric (sometimes spherical) grains (Figure 2c). The EDS analyses show that in their chemical composition is Pb, Fe, Mn, P, Ca, Al and Si (Figure 3a–c). The associations of Mn-Fe oxides and synthetic spherical forms composed of aluminosilicate glass are a distinguishing feature (Figure 2c). In its composition, minerals which due to Pb and P bands in the EDS spectrum, can be classified as Pb phosphates, are present (Figure 3b). Among polymineralic aggregates, grains with Pb, Zn, Mn, Fe, Si, Ca, Mn, and Al in chemical composition occur (Figure 3c). They are common, and the diverse chemical formulas indicate that they are not stable phases. Submicroscopic-size (up to 50 μm in) Ba sulphate grains (Figure 2d,e), occur in association with oxides and Pb carbonates. Crystalline grains of the sulphate can be found (Figure 2e). Barite also occurs as isometric, spherical aggregates with traces of melting at its surface, which is typical for metallurgical pyrolysis processes (Figure 2d). Of particular interest are aggregates with chemical composition and structural features, indicating that they were formed due to high-temperature smelting processes. These are slags produced by medieval smelting industry. These aggregates reach several to several hundred microns in size (Figure 4a). The needle type structures and tabular inclusions (needle form) in mass are characteristic. Needle and tabular forms are built of unstable phases, represented by Ca silicates and aluminosilicates, with Pb, Zn and Fe in their chemical composition. The slag matrix is composed of Pb oxides (litharge) and Ca and Mg (alumino) silicates. In slags, the metallic Pb can be found (Figure 4b). It forms spherical nodules with a thin layer of Pb carbonates on the surface.

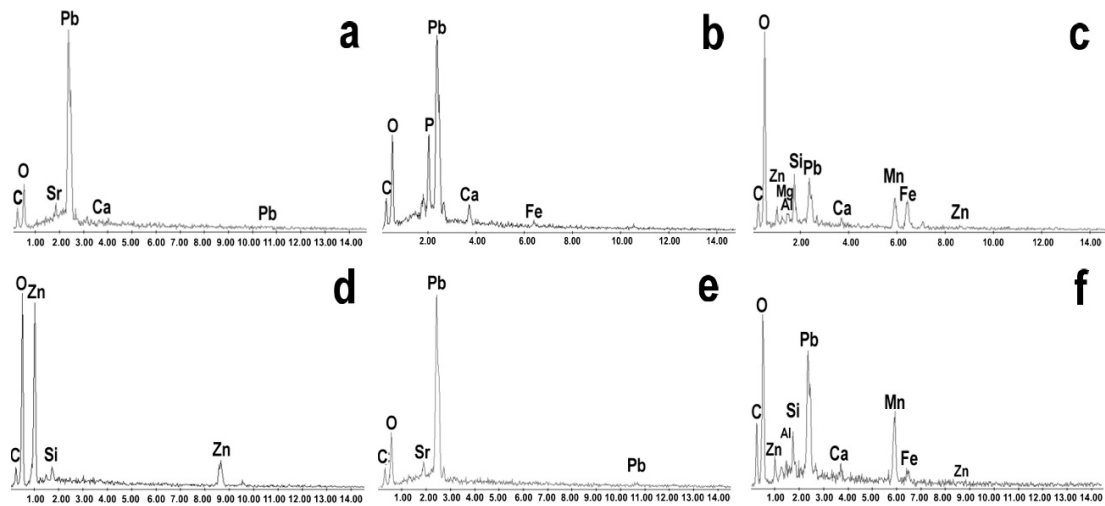


Figure 3. EDS spectra of minerals. Site of archaeological investigation in medieval smelter areas (LO): (a) Pb-oxide (b) Pb-phosphate (c) polymineral aggregates; Pb- and Zn-carbonate, Mn- and Fe-oxide, aluminosilicate. Site of the Zn-Pb ore washing process, area Kawa (KA): (d) Zn-carbonate, (e) Pb-carbonate, (f) aggregated Pb- and Zn-carbonate, Mn- and Fe-oxide, aluminosilicates.

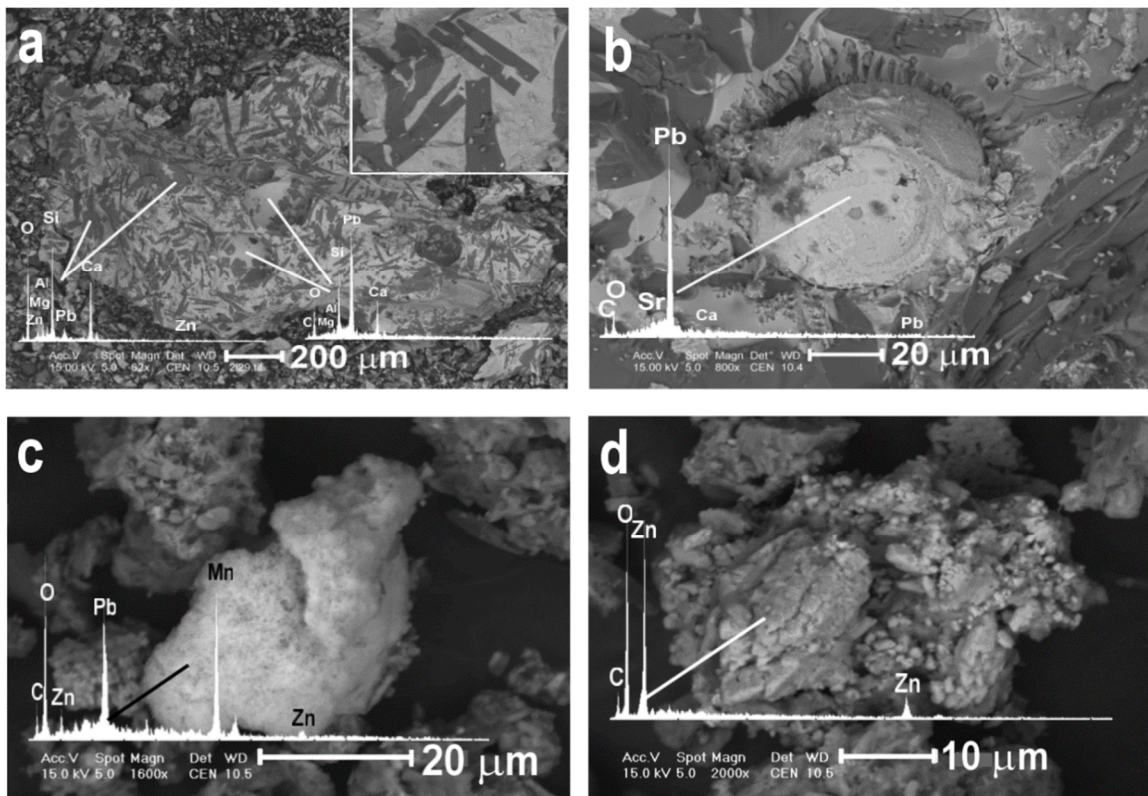


Figure 4. BSE images of metal components in the topsoil. Site archaeological investigations of medieval Ag-Pb smelting operations in Łosień: (a) lead slag in skull form (b) lead slag in Ca-Aluminosilicate matrix. Site Zn-Pb processing operation in Kawa: (c) Aggregate Pb, Zn carbonate and Mn oxide (d) Zn carbonate.

Areas of historical Zn-Pb-Ag ore processing (Kawa)

In soils collected from historical locations of oxidized Zn-Pb ore processing (e.g., muds) (from supergene type Zn-Pb ores) in the surface layers, numerous mineral grains including Pb, Zn, Fe, and Ba in their chemical composition can be identified. Galena and cerussite are the main Pb minerals. Cerussite grains are often covered by Mn oxides (Figure 4c). Next to it is fine-grained Zn and Zn-Mn carbonates, smithsonite and minrecordite are present. Zinc was identified in smithsonite mostly (Figures 3d and 4d). The primary Zn sulphide was not detected. Zinc was found in submicroscopic aggregates formed by aluminosilicates, dolomites, Pb carbonates and Mn and Fe oxides (Figure 3f). Fine-grained (up to 10 μm in size) aggregates composed of grains represented by characteristic assemblage: galena-cerussite-smithsonite-goethite-Mn oxides.

4.2. Slags Phase Chemistry

In the examined slag samples, it was possible to directly analyse changes that the ore minerals (Figure 5a) and smelting process products (Figure 5b) have undergone. In slags, the ore minerals represented by galena (PbS, Table 2) with a chemical composition close to the ideal formula are preserved. It occurs as relics up to 50 μm in size in the metallic lead grains, up to 500 μm in size (Figure 5a and Table 2). On the border with pores, this phase is replaced by litharge (PbO, Table 2). They are accompanied by phases resulting from the smelting process and represented by Ca and Pb silicates, as well as aluminosilicates and glass. Among them are tabular melilite, up to 300 μm in size, was distinguished (Figure 5a). Chemically, it belongs to the åkermanite ($\text{Ca}_2\text{MgSi}_2\text{O}_7$)–gehlenite ($\text{Ca}_2\text{Al}(\text{AlSi})\text{O}_7$) solid solution series whereby the magnesium member is dominating (åk₇₁, Table 3). Moreover, it accumulates Pb (6.34–8.61 wt.% of PbO; Table 3) and Zn (5.54–6.24 wt.% of ZnO; Table 3). The second of the identified phases is probably the lead analogue of larnite (ideally Ca_2SiO_4). In the examined slags it forms needle-like, dendritic crystals up to 300 μm in length or it crystallizes on the melilite surface as tabular crystals up to 200 μm in length (Figure 5a). It concentrates lead (53.53–55.82 wt.% of PbO), so its chemical formula can be presented as $\text{Ca}_{1.02-1.30}\text{Pb}_{0.73-0.89}\text{Si}_{0.96-1.00}\text{O}_4$ (Table 3). Together with these crystals, two types of residual glass occur. Its chemical composition depends of minerals occurring in the vicinity. Type I glass fills large (up to 500 μm in size) spaces between melilite crystals and co-occurs with dendritic Pb-larnite, while type II forms small (up to 20 μm in size) concentrations among tabular melilite and the accompanying Pb-larnite (Figure 5a). Chemically, both types are dominated by Pb (46.72–63.23 wt.% of PbO), Si (20.04–25.75 wt.% of SiO_2), Ca (6.03–14.31 wt.% of CaO), Al (3.60–4.38 wt.% of Al_2O_3) and Fe (2.04–2.61 wt.% of FeO) (Table 3). Type I is characterized by a higher content of Ca, Si, Zn, and Mg, while type II is more concentrate with Pb and Al (Table 3).

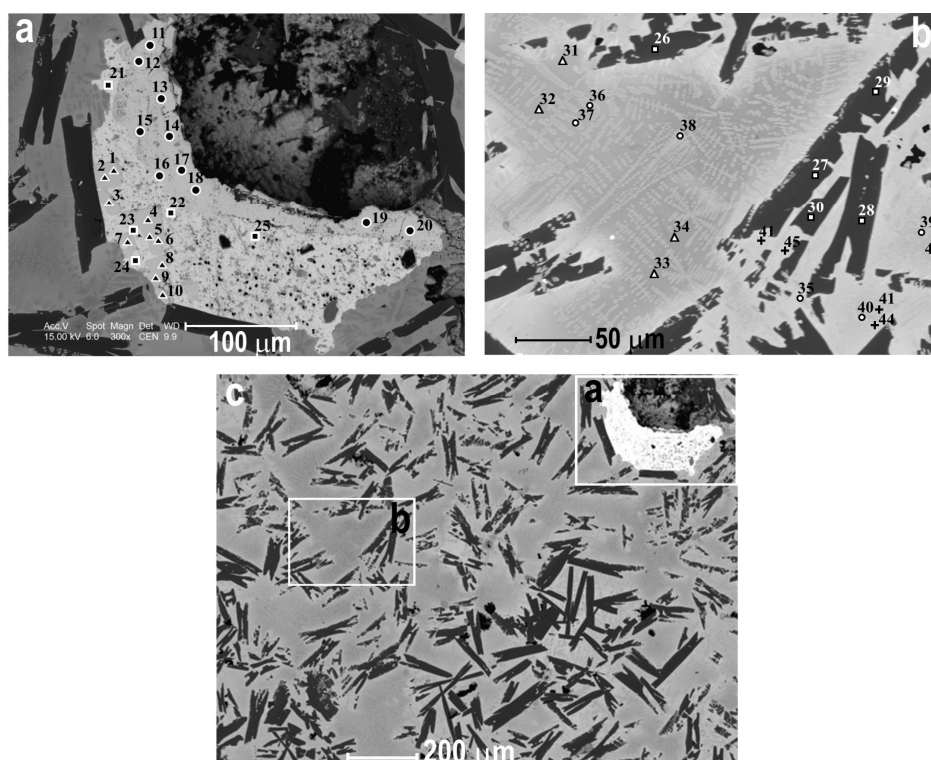


Figure 5. SEM images of slag samples (a) galena, litharge and metallic lead, (b) glass, melilite, lead analogue of larnite. (c) location of area a and b. Points no.—site of EPMA microanalysis specified in Tables 2 and 3. Black triangles—galena, black circles—litharge, black squares—metallic lead, white squares—melilite, white circles—lead analogue of larnite, crosses—glass.

Table 2. Electronprobe microanalyses of phases-building aggregates of relict ore minerals after a smelting process (in wt.%).

| Phase | Analysis No. | Pb | S | O | Total |
|---------|--------------|--------|-------|------|--------|
| Gn | 1 | 86.58 | 13.57 | nd | 100.20 |
| Gn | 2 | 86.97 | 13.39 | nd | 100.48 |
| Gn | 3 | 86.05 | 13.54 | nd | 99.68 |
| Gn | 4 | 87.14 | 13.47 | nd | 100.64 |
| Gn | 5 | 87.74 | 13.45 | nd | 101.20 |
| Gn | 6 | 87.93 | 13.38 | nd | 101.35 |
| Gn | 7 | 86.45 | 13.26 | nd | 99.72 |
| Gn | 8 | 86.63 | 13.44 | nd | 100.09 |
| Gn | 9 | 87.58 | 13.37 | nd | 100.96 |
| Gn | 10 | 87.52 | 13.86 | nd | 101.45 |
| Lit | 11 | 93.40 | nd | 7.21 | 100.61 |
| Lit | 12 | 93.74 | nd | 7.23 | 100.98 |
| Lit | 13 | 93.71 | nd | 7.23 | 100.95 |
| Lit | 14 | 94.86 | nd | 7.32 | 102.18 |
| Lit | 15 | 94.71 | nd | 7.31 | 102.02 |
| Lit | 16 | 94.00 | nd | 7.25 | 101.26 |
| Lit | 17 | 93.08 | nd | 7.18 | 100.27 |
| Lit | 18 | 93.13 | nd | 7.19 | 100.32 |
| Lit | 19 | 92.35 | nd | 7.13 | 99.48 |
| Lit | 20 | 92.56 | nd | 7.14 | 99.70 |
| met. Pb | 21 | 100.66 | nd | nd | 100.66 |
| met. Pb | 22 | 99.86 | nd | nd | 99.86 |
| met. Pb | 23 | 100.97 | nd | nd | 100.97 |
| met. Pb | 24 | 100.93 | nd | nd | 100.93 |
| met. Pb | 25 | 100.05 | nd | nd | 100.05 |

Abbreviations: gn—galena; lit—litharge; met. Pb—metallic lead; nd—not detected.

Table 3. EPMA analyses of silicates, aluminosilicates, and glass building investigated slags (wt.%).

| Phase | mel | mel | mel | mel | mel | gls | gls | gls | gls | Pb-lar | Pb-lar | Pb-lar | Pb-lar | Pb-lar | Pb-lar | gls | gls | gls | gls | gls |
|--|-------|-------|-------|-------|-------|-------|-------|-------|-------|--------|--------|--------|--------|--------|--------|-------|-------|-------|-------|-------|
| Analysis no | 26 | 27 | 28 | 29 | 30 | 31 | 32 | 33 | 34 | 35 | 36 | 37 | 38 | 39 | 40 | 41 | 42 | 43 | 44 | 45 |
| SO ₃ | b.d. | b.d. | 0.04 | b.d. | b.d. | 0.06 | 0.07 | 0.02 | 0.04 | b.d. | b.d. | b.d. | b.d. | b.d. | b.d. | 0.12 | 0.04 | 0.03 | 0.01 | 0.17 |
| P ₂ O ₅ | 0.13 | 0.03 | 0.10 | 0.12 | 0.07 | 0.46 | 0.57 | 0.75 | 0.50 | 1.66 | 1.67 | 1.89 | 1.15 | 2.73 | 1.24 | 0.32 | 0.30 | 0.26 | 0.43 | 0.22 |
| SiO ₂ | 36.71 | 37.11 | 38.36 | 37.16 | 37.65 | 23.53 | 24.17 | 24.99 | 25.75 | 18.17 | 18.88 | 18.92 | 19.67 | 18.13 | 18.13 | 20.65 | 22.64 | 23.28 | 20.60 | 20.40 |
| Al ₂ O ₃ | 4.50 | 4.47 | 3.49 | 4.56 | 4.07 | 3.67 | 3.83 | 3.60 | 3.92 | 0.01 | b.d. | 0.02 | 0.59 | 0.41 | 0.62 | 4.38 | 4.22 | 4.11 | 3.75 | 4.30 |
| CaO | 32.95 | 33.50 | 34.42 | 33.59 | 33.85 | 12.25 | 12.45 | 14.31 | 13.85 | 21.33 | 23.28 | 23.79 | 21.09 | 20.60 | 17.34 | 6.85 | 9.40 | 9.28 | 8.17 | 6.03 |
| PbO | 8.61 | 6.82 | 6.34 | 8.04 | 6.55 | 52.00 | 50.51 | 47.51 | 46.72 | 58.25 | 54.62 | 53.53 | 55.59 | 55.82 | 60.40 | 61.72 | 55.39 | 56.59 | 62.86 | 63.23 |
| MgO | 5.77 | 5.67 | 6.68 | 5.99 | 5.88 | 1.38 | 1.56 | 1.81 | 1.97 | 0.02 | 0.12 | 0.13 | 0.26 | 0.19 | 0.07 | 0.08 | 1.16 | 0.74 | 0.15 | 0.11 |
| FeO | 1.98 | 2.20 | 1.53 | 1.76 | 2.09 | 2.26 | 2.54 | 2.40 | 2.36 | 0.24 | 0.26 | 0.22 | 0.37 | 0.60 | 0.44 | 2.61 | 2.59 | 2.25 | 2.04 | 2.15 |
| MnO | 0.27 | 0.39 | 0.25 | 0.32 | 0.33 | 0.24 | 0.23 | 0.37 | 0.21 | 0.09 | 0.03 | 0.07 | 0.05 | 0.14 | n.d. | 0.20 | 0.27 | 0.23 | 0.12 | 0.16 |
| ZnO | 5.54 | 6.24 | 5.96 | 5.91 | 5.89 | 1.22 | 1.36 | 1.52 | 1.84 | 0.07 | 0.02 | 0.18 | 0.33 | 0.26 | n.d. | 0.22 | 1.07 | 0.42 | 0.14 | 0.24 |
| K ₂ O | 0.33 | 0.72 | 0.59 | 0.30 | 0.79 | 0.48 | 0.59 | 0.49 | 0.58 | 0.22 | 0.22 | 0.23 | 0.21 | 0.31 | 0.25 | 0.68 | 0.59 | 0.58 | 0.61 | 0.63 |
| Ag | b.d. | b.d. | b.d. | b.d. | b.d. | b.d. | b.d. | b.d. | b.d. | b.d. | b.d. | b.d. | b.d. | b.d. | b.d. | b.d. | b.d. | b.d. | b.d. | b.d. |
| Total | 96.79 | 97.15 | 97.76 | 97.75 | 97.17 | 97.55 | 97.88 | 97.77 | 97.74 | 100.06 | 99.10 | 98.98 | 99.31 | 99.19 | 98.49 | 97.83 | 97.67 | 97.77 | 98.88 | 97.64 |
| a.p.f.u. (atoms per formula unit) | | | | | | | | | | | | | | | | | | | | |
| SO ₃ | 0.00 | 0.00 | 0.00 | 0.00 | 0.00 | | | | | 0.00 | 0.00 | 0.00 | 0.00 | 0.00 | 0.00 | | | | | |
| P ₂ O ₅ | 0.00 | 0.00 | 0.00 | 0.00 | 0.00 | | | | | 0.00 | 0.00 | 0.00 | 0.00 | 0.00 | 0.00 | | | | | |
| SiO ₂ | 1.92 | 1.92 | 1.95 | 1.92 | 1.94 | | | | | 0.96 | 0.97 | 0.96 | 1.00 | 0.96 | 1.00 | | | | | |
| Al ₂ O ₃ | 0.28 | 0.27 | 0.21 | 0.28 | 0.25 | | | | | 0.00 | 0.00 | 0.00 | 0.04 | 0.03 | 0.04 | | | | | |
| CaO | 1.85 | 1.85 | 1.87 | 1.86 | 1.86 | | | | | 1.21 | 1.28 | 1.30 | 1.14 | 1.17 | 1.02 | | | | | |
| PbO | 0.12 | 0.09 | 0.09 | 0.11 | 0.09 | | | | | 0.83 | 0.75 | 0.73 | 0.76 | 0.80 | 0.89 | | | | | |
| MgO | 0.45 | 0.44 | 0.51 | 0.46 | 0.45 | | | | | 0.00 | 0.01 | 0.01 | 0.02 | 0.02 | 0.01 | | | | | |
| FeO | 0.09 | 0.10 | 0.07 | 0.08 | 0.09 | | | | | 0.01 | 0.01 | 0.01 | 0.02 | 0.03 | 0.02 | | | | | |
| MnO | 0.01 | 0.02 | 0.01 | 0.01 | 0.01 | | | | | 0.00 | 0.00 | 0.00 | 0.00 | 0.01 | 0.00 | | | | | |
| ZnO | 0.21 | 0.24 | 0.22 | 0.23 | 0.22 | | | | | 0.00 | 0.00 | 0.01 | 0.01 | 0.01 | 0.00 | | | | | |
| K ₂ O | 0.02 | 0.05 | 0.04 | 0.02 | 0.05 | | | | | 0.01 | 0.01 | 0.01 | 0.01 | 0.02 | 0.02 | | | | | |
| Ag | 0.00 | 0.00 | 0.00 | 0.00 | 0.00 | | | | | 0.00 | 0.00 | 0.00 | 0.00 | 0.00 | 0.00 | | | | | |
| Total | 4.95 | 4.97 | 4.96 | 4.96 | 4.97 | | | | | 3.04 | 3.04 | 3.04 | 2.99 | 3.04 | 2.99 | | | | | |

Abbreviations: gls—glass; mel—melilite; Pb-lar—lead analogue of larnite; b.d.—below detection limit. 4.3. Slag Melting Point.

As a consequence of heating, slags have undergone the following changes: (i) after heating in temperatures of up to 1150 °C, the colour of the slags changed to rusty-red; the morphology of slag did not change (Figure 6b); (ii) heating up to between 1250 °C and 1350 °C, caused changes of slag surface morphology to more oval as a result of local eutectics occurrences (Figure 6c,d); (iii) after heating in the temperature of up to 1450 °C, partial melting of the sample with separation of the liquid took place, while some part of the sample had not been melted (Figure 6e); (iii) after heating up to 1550 °C, the slag sample was completely melted (Figure 6f).

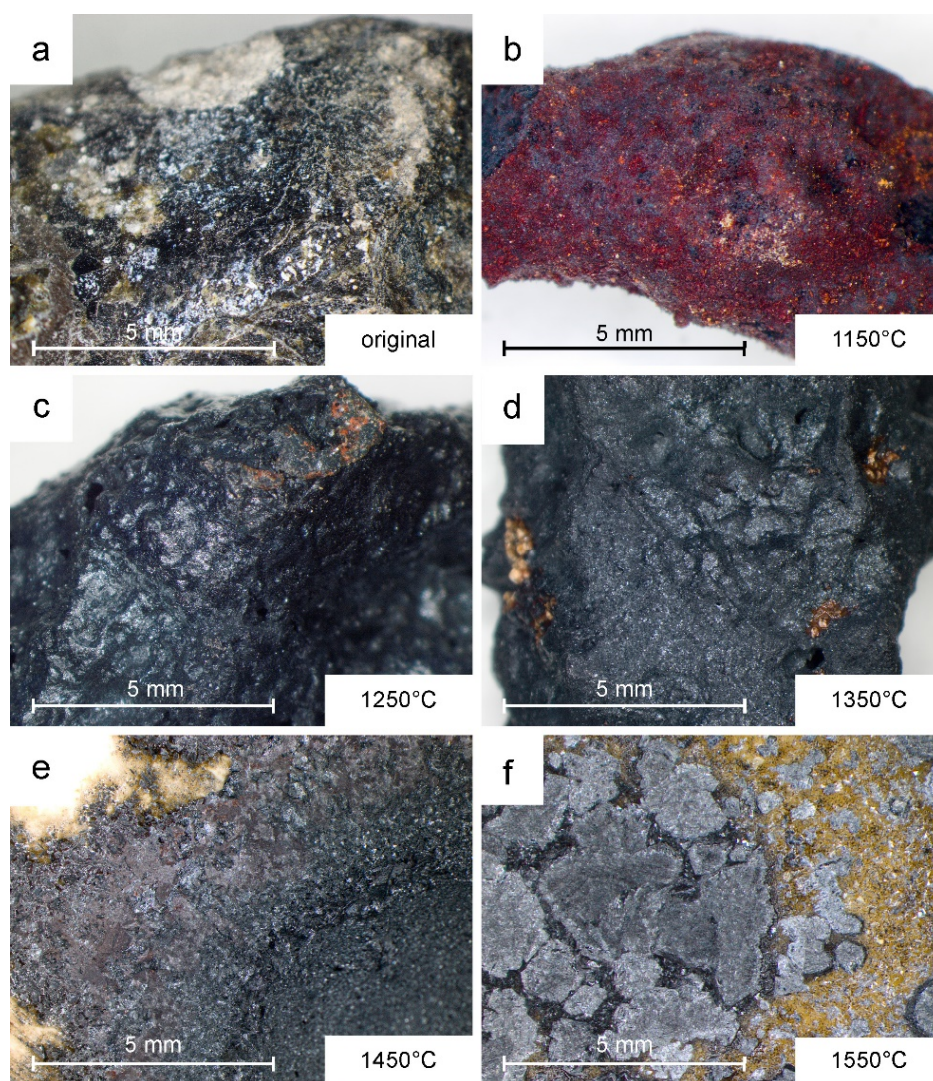


Figure 6. Macrophotographs of slag from Łosień before (a) and after heating experiments in temperatures of: (b) 1150 °C; (c) 1250 °C; (d) 1350 °C; (e) 1450 °C; (f) 1550 °C.

4.3. Heavy Metals in Topsoil from Historical Processing Areas

Atomic Absorption Spectroscopy (AAS) analyses of topsoil individual fractions (LO samples) shows that after finishing archaeological works and levelling the ground, in the soil surface layer, a higher concentration of Pb and Fe is clearly distinguishable (Table 4). Submicroscopic grains enriched in Pb and Fe are concentrating in the smallest fractions: 0.09–0.045 mm and <0.045 mm. The level of Zn concentration is noticeably lower. The content of Cd in the smallest fractions reaches up to 4.7 mg·kg⁻¹ (Table 4). In the area of former Zn-Pb-Ag ore mud the level of Zn, Pb, Fe, Mn and Cd concentration is extremely high in all of the top-soil fractions j (KA samples). Cd up to 287 mg·kg⁻¹, Zn up to 64,408 mg·kg⁻¹, and Pb up to 49,282 mg·kg⁻¹ (Table 4) contents are especially high.

Table 4. Metals concentration in topsoil fraction from historical smelting (Łosień—LO) and processing operation (Kawa—KA). Five samples were collected in each location (see: Sampling).

| Samples | Fraction mm | Zn | Pb | Fe | Mn | Cd |
|---|----------------|---------------------------|-------------------|-------------------|---------------|-------------|
| | | mg·kg ⁻¹ (STD) | | | | |
| Sites polluted by archeological investigations in areas of 12th century Ag-Pb smelting (Łosień) | | | | | | |
| LO | >0.71 | 287.5 (53) | 306.0 (206) | 9292.2 (779) | 422.1 (32) | 0.5 (0.5) |
| LO | >0.355 | 197.2 (27) | 861.6 (756) | 6544.5 (566) | 307.6 (39) | 0.4 (0.4) |
| LO | >0.180 | 189.1 (28) | 192.0 (137) | 6814.8 (331) | 305.5 (22) | 0.9 (1.1) |
| LO | >0.09 | 399.9 (21) | 549.6 (199) | 14,015.2 (910) | 691.9 (40) | 2.6 (0.5) |
| LO | >0.045 | 782.5 (88) | 1106.5 (304) | 21,713.5 (2847) | 1077.7 (144) | 4.7 (1.6) |
| LO | <0.045 | 557.4 (99) | 833.7 (6) | 16,328.4 (3470) | 719.5 (313) | 3.4 (1.7) |
| Sites polluted by Zn-Pb historical washing and mining processes (Kawa) | | | | | | |
| KA | >0.71 | 49,257.6 (32,175) | 18,923.0 (3356) | 49,676.9 (2314) | 2718.4 (1967) | 251.6 (91) |
| KA | >0.355 | 36,737.6 (8629) | 10,960.6 (8074) | 54,764.1 (18,358) | 2642.4 (1833) | 136.4 (52) |
| KA | >0.180 | 41,658.8 (10,600) | 12,980.5 (9446) | 59,389.5 (22,184) | 2869.4 (2102) | 137.7 (48) |
| KA | >0.09 | 64,408.7 (29,984) | 26,847.9 (22,520) | 72,722.6 (14,175) | 3208.8 (2046) | 219.9 (113) |
| KA | >0.045 | 58,352.1 (46,242) | 49,282.5 (51,362) | 70,620.7 (25,510) | 4297.7 (3884) | 287.1 (180) |
| KA | <0.045 | 16,917.5 (18,155) | 26,622.1 (33,426) | 43,437.3 (14,183) | 2326.9 (721) | 207.3 (164) |

5. Discussion

Locations in which silver and lead melting furnaces operated in the medieval period are contaminated by metal-bearing mineral phases with elements occurring in the ores used to smelt lead and silver. In the area of Silesian-Cracov Zn-Pb-Ag ore deposits, these elements are Zn, Pb, Fe, Cd, Tl, Mn, Ba, and As [30,31].

From the topsoil, formed after several years of archaeological work, it was possible to separate metal-bearing (Zn, Pb, Fe, Cd) grains and mineral aggregates (from 20 µm to 5 mm in size). This have included primary or synthetic phases, which are derived from lead and silver production batches or medieval smelting products. The level of Pb concentration in all fractions of the studied soil is higher than the amount of Zn. It shows that enriched (e.g. in muds) galena ores with relatively low Zn content was in the batch for the melting furnaces. The highest amount of metals was noted in the fractions >0.045 to 0.09 mm (Table 4).

The metal-bearing phases associated with medieval metallurgy came from an archaeologically examined cultural layer, in which next to the slags, fragments of glazed ceramics, lead and silver lumps, silver coins, ornaments and utility goods were found [3,5,32]. The lead smelting processes were based on Zn-Pb-Ag ores of the MVT-type. A characteristic feature is the occurrence of mineral assemblage represented by synthetic and primary and secondary minerals: Aluminosilicate glass, Metallic Pb, Pb oxide (litharge), Cerussite, Barite, and aluminosilicate aggregate with Pb, Phosphate, and Fe and Mn oxide.

Among the metal-bearing minerals, a significant feature is the participation of secondary phases, which have been formed over a period of 800 years as a result of metallurgical slag weathering. Geochemical transitions have caused resulted in secondary phases enriched in Zn and Pb, which are formed at the surface of pyrolytic transformations products. Microcracks in the minerals grains show signs of lixiviation and porous carbonate aggregates disintegrate and are partially dissolved.

A similar type of transformation connected with acid mine drainage (AMD) was observed in the Freiberg area (Germany), in the wastes from historical mining industry [25]. They could have had impact on metal transfer (e.g., Zn, Pb, Cd, As) to the environment. In the medieval lead metallurgical processing sites in Great Britain, a similar mineral group represented by litharge, cerussite, pyromorphite with the association of unstable phases, like Ca silicates, Si glass, and barite, was identified [33]. The described assemblage shows that in a medieval (12th century) smelter, locally available Zn-Pb ore materials were used for metallurgical production of lead and litharge. In the

12th century in the whole area, lead production was significant, so both lead and its compounds was probably subject to trade in the Central and Eastern Europe. This is confirmed by the research of Ettlér et al. [11], which shows that the litharge isotopic signature from Prague area (Czech Republic), indicates that it was produced from galena in the Silesian-Cracow Zn-Pb ore deposits.

The obtained results can be used to approximate the metallurgical process in the sampled location. On the basis of conducted furnace experiments, it has been confirmed that the temperature of smelting had been up to 1550 °C. Such high temperatures are not characteristic for more contemporary methods of Pb and Zn smelting, where they are in the 1000–1300 °C temperature range [34]. Studies show that such high temperatures could be obtained by using tuyeres in the furnace design [35].

They are compatible with the described mineral compositions in which Ca-rich phases (melilite, Pb-larnite) are dominant. These can be responsible for the raising of the melting point [36]. This points out a low-quality ore enrichment process in which a large amount of dolomite gangue has not been removed. Similar phases were described by Ettlér et al. [11] in early-medieval slags from the Na Slupi site (Prague, Czech Republic). Its red variety includes glass, larnite, and Pb silicate (Pb_2SiO_4), melilite, kalsilite and wollastonite. The lack of Ag in slag building phases indicates a high efficiency of the silver recovery process.

Unlike the examined samples, slags from Czech Republic contain metallic copper as well. At the same time, they are different from Bohutín (Czech Republic) or Massa Marittima (Italy) slags, which did not include calcium phases in such large quantities [27,28]. This fact is reflected in the melting temperatures, estimated at 800–1200 °C in Bohutín's case [27] and 1150–1300 °C in Massa Marittima [28]. It is worth noting that slags from Bohutín and Massa Marittima are younger (14th century), so they can be a result of a more advanced enrichment and smelting process. The occurrence of galena in the Łosień material suggests at least the partial use of sulfide ores during the smelting process, which took place in a reducing environment, making it possible to obtain metallic lead. Based on the samples collected, it is difficult to indicate if the reducing environment was obtained by using wood or charcoal. At the same time, the presence of galena indicates that the ores were not roasted before smelting, which would result in its oxidation. The occurrence of litharge, which was detected in the slags, is limited to the immediate vicinity of pores, which suggest that it was formed probably as a result of secondary metallic lead oxidation. A separate issue is the dominance of silicate phases in the slags, while this element is not common in the MVT ores of the Silesia-Cracow area. Descriptions of similar historical processes [37], did not clearly indicate its origin in the slags, however, they suggested that the slag itself was repeatedly used in the metallurgical process to bind impurities, which can affect the purity of the resulting melt. During the furnace start-up period, if the slags from earlier smelting were not available, quartz sand was added for this purpose, which was easily accessible at the examined area. Quartz grains observed by Ettlér et al. [11] in historically related material from Prague can be considered confirmation of this.

6. Summary and Conclusions

The analysis of former Pb-Ag metallurgic products chemistry, environmental paleocontamination, and the reconstruction of metal production methods is now possible due to the application of mineralogical, geochemical, and environmental research. Soil research from the investigated archaeological sites showed that chemical (AAS) and mineralogical (XRD, SEM, EPMA) methods are useful for identifying the former Pb-Ag metallurgical site.

Places of archaeological work, in which smelting furnaces were identified, landfills or old ore mud are particularly well-suited for conducting mineralogical and geochemical research aimed at the determination of the metallurgical activity type, ore chemical composition and type of products obtained after its processing.

The identification of synthetic aggregates provides clear evidence of soil contamination by metallurgical and processing wastes in Łosień and Kawa sites. These submicroscopic size, polymineral

aggregates with Pb, Zn, Mn, Fe, Si, Ca, Mn, and Al carbonates and sulfates were formed in the oxidation zone.

Chemical analyses of sieved samples proved that the concentration of these aggregates is dependent on the soil fraction. The highest concentrations of Pb, Zn, Fe Cd, and Ag were distinguished fine-grained soil fractions (>0.045 to 0.09 mm).

The application of an experimental approach together with mineralogical investigations allows for the reconstruction of historical smelting processes. The result presented herein confirmed: (i) the usage of sulfide type ores, (ii) usage of additives in the process (probably quartz sand), (iii) reductive conditions during smelting and oxidative during slag crystallization, (iv) melting temperature of ca. 1550 °C, and (v) the efficiency of silver recovery.

Author Contributions: Conceptualization, J.C. and R.W.; methodology, J.C., R.W. and D.R.; formal analysis, J.C., R.W., D.R., E.S.; investigation, J.C., R.W., D.R., E.S.; resources, J.C. and R.W.; writing—original draft preparation, J.C. and R.W.; writing—review and editing, J.C., R.W. and D.Ś.; visualization, J.C. and R.W.; supervision, J.C.; project administration, J.C.; funding acquisition, R.W. All authors have read and agreed to the published version of the manuscript.

Funding: This research was funded by National Science Center (NCN), grant number 2016/21/N/ST10/00838.

Conflicts of Interest: The authors declare no conflict of interest.

References

1. Heijlen, W.; Muchez, P.H.; Banks, D.A.; Schneider, J.; Kucha, H.; Keppens, E. Carbonate-hosted Zn-Pb deposits in Upper Silesia, Poland: Origin and evolution of mineralizing fluids and constraints on genetic models. *Econ. Geol.* **2003**, *98*, 911–932. [[CrossRef](#)]
2. Boni, M.; Large, D. Nonsulfide zinc mineralization in Europe: An overview. *Econ. Geol.* **2003**, *98*, 715–729. [[CrossRef](#)]
3. Rozmus, D. *Early Medieval District of Silver and Lead Metallurgy in the Frontier Areas of Upper Silesia Little Poland/second half of the 11th–12th/13th Centuries*; City Museum “Sztygarka” and Academic Publishing House: Kraków, Poland, 2014; p. 317.
4. Karbowniczek, M.; Suliga, I.; Bodnar, R.; Szmoniewski, B.S. An Attempt of Reproduction of the Medieval Technology of Lead Metallurgy. In *Frühmittelalterliche glasierte Keramik aus Łosień. “Der Schatz des Metallschmelztes”*; Rozmus, D., Szmoniewski, B.S., Eds.; Academic Publishing House: Kraków, Poland, 2006; pp. 36–40.
5. Rozmus, D.; Szmoniewski, B.S. Did the advancement of early mediaeval technology of silver and lead smelting cause pollution? A case study of the Łosień - Strzemieszyce region. *Acta Rerum Naturalium.* **2013**, *16*, 203–216.
6. Tylecote, R.F. The effect of soil conditions on the long-term corrosion of buried tin-bronzes and copper. *J. Archeol. Sci.* **1979**, *6*, 345–368. [[CrossRef](#)]
7. Bachmann, H.G. *The Identification of Slags from Archeological Sites*; Routledge: London, UK, 2016.
8. Magiera, T.; Mendakiewicz, M.; Szuskiewicz, M.; Jabłońska, M.; Chróst, L. Technogenic magnetic particles in soils as evidence of historical mining and smelting activity: A case of the Brynica River Valley, Poland. *Sci. Total Environ.* **2016**, *566*, 536–551. [[CrossRef](#)]
9. Potysz, A.; Kierczak, J.; Grybos, M.; Pędziwiatr, A.; van Hullebusch, E.D. Weathering of historical copper slags in dynamic experimental system with rhizosphere-like organic acids. *J. Environ. Manage.* **2018**, *222*, 325–337. [[CrossRef](#)]
10. Dill, H.G. Pyrometallurgical relics of Pb–Cu–Fe deposits in south-eastern Germany: An exploration tool and a record of mining history. *J. Geochem. Explor.* **2009**, *100*, 37–50. [[CrossRef](#)]
11. Ettler, V.; Johan, Z.; Zavrel, J.; Selmi Wallisova, M.; Mihaljevic, M.; Sebek, O. Slag remains from the Na Slupí site (Prague, Czech Republic): Evidence for early medieval non-ferrous metal smelting. *J. Archeol. Sci.* **2015**, *53*, 72–83. [[CrossRef](#)]
12. De Caro, T. The ancient metallurgy in Sardinia (Italy) through a study of pyrometallurgical materials found in the archaeological sites of Tharros and Montevecchio (West Coast of Sardinia). *J. Cult. Herit.* **2017**, *28*, 65–74. [[CrossRef](#)]

13. Warchulski, R.; Juszczuk, P.; Gawęda, A. Geochemistry, petrology and evolutionary computations in the service of archaeology: restoration of the historical smelting process at the Katowice–Szopienice site. *Archaeol. Anthropol. Sci.* **2018**, *10*, 1023–1035. [[CrossRef](#)]
14. Portillo, H.; Zuluaga, M.C.; Ortega, L.A.; Alonso-Olazabal, A.; Murelaga, X.; Martinez-Salcedo, A. XRD, SEM/EDX and micro-Raman spectroscopy for mineralogical and chemical characterization of iron slags from the Roman archaeological site of Forua (Biscay, North Spain). *Microchem. J.* **2018**, *138*, 246–254. [[CrossRef](#)]
15. Álvarez-Valero, A.M.; Pérez-López, R.; Nieto, J.M. Prediction of the environmental impact of modern slags: A petrological and chemical comparative study with Roman age slags. *Am. Mineral.* **2009**, *94*, 1417–1427. [[CrossRef](#)]
16. Piatak, N.M.; Seal II, R.R. Mineralogy and the release of trace elements from slag from the Hegeelr Zinc smelter, Illinois (USA). *Appl. Geochem.* **2010**, *25*, 302–320. [[CrossRef](#)]
17. Tyszka, R.; Kierczak, J.; Pietranik, A.; Ettler, V.; Mihajević, M. Extensive weathering of zinc smelting slag in a heap in Upper Silesia (Poland): Potential environmental risks posed by mechanical disturbance of slag deposits. *Appl. Geochem.* **2014**, *40*, 70–81. [[CrossRef](#)]
18. Warchulski, R.; Gawęda, A.; Janeczek, J.; Kaździółka-Gaweł, M. Mineralogy and origin of coarse-grained segregations in the pyrometallurgical Zn–Pb slags from Katowice–Wełnowiec (Poland). *Miner. Petrol.* **2016**, *110*, 681–692. [[CrossRef](#)]
19. Saikia, N.; Borah, N.N.; Konwar, K.; Vandecasteele, C. pH dependent leachings of some trace metals and metalloid species from lead smelter slag and their fate in natural geochemical environment. *Groundw. Sustainable Development.* **2018**, *7*, 348–358. [[CrossRef](#)]
20. Warchulski, R.; Mendecki, M.; Gawęda, A.; Sołtysiak, M.; Gadowski, M. Rainwater-induced migration of potentially toxic elements from a Zn–Pb slag dump in Ruda Śląska in light of mineralogical, geochemical and geophysical investigations. *Appl. Geochem.* **2019**, *109*, in press. [[CrossRef](#)]
21. Merrington, G.; Alloway, B.J. The transfer and fate of Cd, Cu and Zn from two historic metalliferous mine sites in the UK. *Appl. Geochem.* **1994**, *9*, 677–687. [[CrossRef](#)]
22. Renberg, I.; Brannvall, M.L.; Bindler, R.; Emteryd, O. Stable lead isotopes and lake sediments—A useful combination for the study of atmospheric lead pollution history. *Sci. Total Environ.* **2002**, *292*, 45–54. [[CrossRef](#)]
23. Sanchez, J.; Marino, N.; Vaquero, M.C.; Ansorena, J.; Lego Rburu, I. Metal pollution by old lead-zinc mines in Urumea River Valley (Basque country, Spain). Soil, biota and sediment. *Water Air Soil Poll.* **1988**, *107*, 303–319. [[CrossRef](#)]
24. Maskall, J.; Whitehead, K.; Gee, C.; Thornton, I. Long-term migration of metals at historical smelting sites. *Appl. Geochem.* **1996**, *11*, 43–51. [[CrossRef](#)]
25. Scheinert, M.; Kupsch, H.; Bletz, B. Geochemical investigations of slags from the historical smelting in Freiberg, Erzgebirge (Germany). *Chem. der Erde* **2009**, *69*, 81–90. [[CrossRef](#)]
26. Mahe-Le Carlier, C.; Ploquin, A.; Fluck, P. Apport de la géochimie et de la pétrologie à la connaissance de la métallurgie primaire du plomb argentifère au Moyen Âge: les exemples du Mont Lozère (Cevennes) et de Pfaffenloch (Vosges). *Archeo. Sciences.* **2010**, *34*, 159–176. [[CrossRef](#)]
27. Ettler, V.; Červinka, R.; Johan, Z. Mineralogy of medieval slags from lead and silver smelting (Bohutín, Příbram district, Czech Republic): towards estimation of historical smelting conditions. *Archaeometry* **2009**, *51*, 987–1007. [[CrossRef](#)]
28. Manasse, A.; Mellini, M. Chemical and textural characterisation of medieval slags from the Massa Marittima smelting sites (Tuscany, Italy). *J. Cult. Herit.* **2002**, *3*, 187–198. [[CrossRef](#)]
29. Viets, J.G.; Leach, D.L.; Lichte, F.E.; Hopkins, R.T.; Gent, C.A.; Powell, J.W. Paragenetic and minor-and trace-element studies of Mississippi Valley-type ore deposits of the Silesian-Cracow district, Poland. *Pr. Inst. Geol.* **1996**, *154*, 51–71.
30. Cabala, J. Development of oxidation in Zn–Pb deposits in Olkusz area. In *Mineral Deposits at the Beginning of the 21st Century*; Piestrzyński, A., Ed.; CNC Press/Balkema: Leiden, The Netherlands, 2001; pp. 121–124.
31. Cabala, J.; Żogała, B.; Dubiel, R. Geochemical and geophysical study of historical Zn–Pb ore processing waste dump areas (Southern Poland). *Pol. J. Environ. Stud.* **2008**, *17*, 693–700.
32. Garbacz-Klempka, A.; Rozmus, D. The “Metallurgist's Hoard”. Silver and Lead Smelting in the Early Medieval Poland. *Arch. Foundry Eng.* **2015**, *15*, 17–20.

33. Gee, C.; Ramsey, M.H.; Maskall, J.; Thornton, I. Mineralogy and weathering processes in historical smelting slags and their effect on the mobilization of lead. *J. Geochem. Explor.* **1997**, *58*, 249–257. [[CrossRef](#)]
34. Warchulski, R. Zn-Pb slag crystallization: Evaluating temperature conditions on the basis of geothermometry. *Eur. J. Mineral.* **2016**, *28*, 375–384. [[CrossRef](#)]
35. Orzechowski, S.; Przychodni, A. Experimental Iron Smelting in the Research on Reconstruction of the Bloomery Process in the Świętokrzyskie (Holy Cross) Mountains, Poland. In *Experiments Past: Histories of Experimental Archaeology*; Reeves Flores, J., Paardekooper, R., Eds.; Sidestone Press: Leiden, The Netherlands, 2014; pp. 249–268.
36. Osborn, E.F.; DeVries, R.C.; Gee, K.H.; Kraner, H.M. Optimum Composition of Blast Furnace Slag as Deduced from Liquidus Data for Quaternary System CaO-MgO-Al₂O₃-SiO₂. *J.O.M.* **1954**, *200*, 33–45. [[CrossRef](#)]
37. Agricola, G. *De Re Metallica*; Dover Publications: New York, NY, USA, 1950.



© 2019 by the authors. Licensee MDPI, Basel, Switzerland. This article is an open access article distributed under the terms and conditions of the Creative Commons Attribution (CC BY) license (<http://creativecommons.org/licenses/by/4.0/>).